

1-1-2010

Immobilization of Motile Bacterial Cells via Dip-pen Nanolithography

Dorjderem Nyamjav
Loyola University Chicago

Sergey Rozhok
Northwestern University

Richard C. Holz
Marquette University

Accepted version. *Nanotechnology*. Vol. 21, No. 23 (2010): 235105. DOI. © Copyright 2019 IOP Publishing. Used with permission.

Richard C. Holz was affiliated with Loyola University-Chicago at the time of publication.

Marquette University

e-Publications@Marquette

Chemistry Faculty Research and Publications/College of Arts and Sciences

This paper is NOT THE PUBLISHED VERSION; but the author's final, peer-reviewed manuscript. The published version may be accessed by following the link in the citation below.

Nanotechnology, Vol. 21, No. 23 (2010): 235105. DOI. This article is © Institute of Physics and permission has been granted for this version to appear in e-Publications@Marquette. Institute of Physics does not grant permission for this article to be further copied/distributed or hosted elsewhere without the express permission from Institute of Physics.

Immobilization of motile bacterial cells via dip-pen nanolithography

Dorjderem Nyamjav

The Department of Chemistry, Loyola University-Chicago, 1068 N. Sheridan Road, Chicago, IL

Sergey Rozhok

The Department of Chemistry and Institute for Nanotechnology, Northwestern University, 2145 Sheridan, Road, Evanston, IL

Richard C Holz

The Department of Chemistry, Marquette University, Milwaukee WI

The Department of Chemistry, Loyola University-Chicago, 1068 N. Sheridan Road, Chicago, IL

Abstract

A strategy to bind bacterial cells to surfaces in a directed fashion via dip-pen nanolithography (DPN) is presented. Cellular attachment to pre-designed DPN generated microarrays was found to be dependent on the shape and size of the surface feature. While this observation is likely due in part to a dense, well formed mercaptohexadecanoic acid (MHA) monolayer generated via DPN, it may also simply be due to the physical shape of the surface structure. Motile *Pseudomonas aeruginosa* bacterial cells were observed to bind to DPN generated mercaptohexadecanoic acid/poly-L-lysine (MHA/PLL) line patterns, 'blocks' made up of eight lines with 100 nm spacings, with ~ 80% occupancy. Cellular binding to these 'block' surface structures occurs via an electrostatic interaction between negatively charged groups on the bacterial cell surface and positively charged

poly-L-lysine (PLL) assemblies. These data indicate that these DPN generated 'block' surface structures provide a promising footprint for the attachment of motile bacterial cells that may find utility in cell based biosensors or single cell studies.

1. Introduction

Developing methods to pattern and immobilize biological molecules with micro- to nanometer scale control has resulted in a broad range of new technological advancements in diagnostics and drug discovery [1–4]. Some of the most interesting and useful advancements have come in the areas of biochip array development that utilize DNA, proteins, or carbohydrates as linker molecules [5, 6]. Patterned substrates have also been used as scaffolds for biomolecule binding, cell adhesion in tissue engineering studies, as well as components for microfluidic bioanalysis [7–9]. However, many challenges remain, particularly the development of patterning methods that combine micro- to nanoscale surface features with adhesion chemistries that not only provide selectivity in biomolecule binding and positioning, but also preserve biological activities. Importantly, unpatterned areas of the surface must resist non-specific biomolecule binding for the effective development of most biological and commercial applications.

As with most bacterial species, pathogenic bacteria exhibit significant variations between strains, including variation in the presence of genes encoding virulence factors, toxins, and antibiotic resistance [10]. Understanding the specific surface binding characteristics of individual pathogenic bacterial strains will potentially enhance the ability to detect, diagnose, and treat bacterial infections, enabling researchers to identify the source of a pathogen and track its spread [9]. Therefore, the ability to selectively bind cells to surfaces in spatially controlled cell binding microarrays may lead to the development of bacterial cell detection devices that will not only detect bacterial pathogens quickly and accurately but will also simultaneously capture these bacterial pathogens in a way that permits further, post-capture analysis [9, 11].

Dip-pen nanolithography (DPN) provides a flexible nanolithographic method capable of positioning molecules on a substrate with 10 nm resolution [12]. DPN can be used to pattern tailored inks on bio-inert substrates, leading to nanoscale positioning of active proteins, virus particles, and cells [13]. This method has the characteristics required to pattern individual motile bacterial cells in surface-derived microarrays or gradients [14]. Herein, we describe the use of DPN to prepare pre-defined surface templates that are used to immobilize motile *Escherichia coli* and *Pseudomonas aeruginosa* bacterial cells. *P. aeruginosa* cells were chosen because this organism is an opportunistic pathogen that can infect the pulmonary tract, urinary tract, burns, and wounds but can also cause ear and blood infections as well as colonize medical devices [15, 16]. Since *P. aeruginosa* cells typically exhibit low susceptibility to antibiotics and *E. coli* O157:H7 is a prime cause of foodborne illnesses, the preparation of well-defined microarrays of both *E. coli* and *P. aeruginosa* cells may lead to the design of improved cellular detection devices. Our data suggest that DPN generated patterns can bind single *E. coli* or *P. aeruginosa* cells, forming pre-designed bacterial microarrays.

2. Materials and methods

2.1. Materials

Hydrogen peroxide (30%) and sulfuric acid were purchased from Fisher Scientific. 16-mercaptohexadecanoic acid (MHA) (90%), 1-octadecanethiol (ODT) (98%), and poly-L-lysine (PLL) (0.01% solution with mol. wt. 70 000–150 000) were purchased from Sigma-Aldrich, Inc. (Milwaukee, WI). All chemicals were used as-received without further purification. Milli-Q water (18.2 M Ω) was used for all aqueous experiments. Gram-rods of *E. coli* K12 were obtained from the Carolina Biological Supply Company while the *P. aeruginosa* bacterial cell culture was provided as a gift from Professor C Harwood at the University of Iowa [17].

2.2. Substrate preparation

Gold substrates were fabricated by thermal evaporation of a layer of gold (30 nm) onto a titanium (10 nm) coated silicon oxide wafer (8 × 12 mm²). Si wafers (4 in, 475–575 mm thickness with a 500 nm thermal oxide layer, Wafernet, Inc. (San Jose, CA)) were cleaned with piranha (3:1 = H₂SO₄:H₂O₂) solution prior to thermal evaporation. (Caution! Piranha solution should be handled carefully as it may cause serious burns.)

2.3. Cell culture preparation

E. coli K-12 and *P. aeruginosa* cells were grown from single colonies in Luria-Bertani (LB) broth (Sigma) in a rotary shaker incubator at 37 °C and 225 rpm for 7–8 h. When the optical density (OD₆₀₀) of the culture reached about 0.5–0.8 (Shimadzu 2450 UV–vis), the bacterial cells were centrifuged at 4000 rpm for 20 min and resuspended in M9 media prepared from commercially available M9 minimal salts (Sigma, Milwaukee). The final bacterial cell concentration was approximately 5 × 10⁷ cells ml⁻¹, which was determined by measuring the absorbance at 600 nm and by cellular counting methods using a Bright-Line hemacytometer (Fisher Scientific).

2.4. Microarray preparation

Initially, substrates were washed in piranha solution at 40 °C for 5 min in order to remove any form of organic contaminant from the gold surface. A NanoInk, Inc. Nscriptor™ was used to prepare DPN MHA microarrays under environmental conditions with temperatures ranging from 20 to 22 °C and humidity levels within the enclosed chamber between 25 and 35%. V-shaped, silicon nitride contact mode tips (model MSCT-AUNM-10, Veeco, Inc.) with a spring constant of 0.05 N m⁻¹ were used for DPN patterning and contact mode imaging. For DPN patterning of MHA on Au surfaces, AFM tips were dipped briefly into a solution of 10 mM MHA in acetonitrile (99.9%; Sigma) and air dried before being mounted onto the Nscriptor™ tip holder. Prior to DPN patterning, the diffusion constants, stationary and/or dynamic, were calculated based on the model developed by Jang *et al* [18] using Nscriptor™ software InkCAD. Dot shaped patterns were made by holding the tip stationary in contact with the surface while DPN generated lines were fabricated by moving the coated tip, with a pre-calculated speed, in contact with the surface.

2.5. Modification of the DPN patterned templates

Substrates with DPN generated MHA patterns were incubated in a 10 mM solution of ODT in ethanol (99.9%; Sigma) for 30 min in order to passivate unpatterned areas. These samples were then rinsed with ethanol and dried under a stream of nitrogen. MHA coated regions were then functionalized using a 0.01% aqueous solution of PLL, rinsed with Milli-Q 18 Ω water and dried under nitrogen. Finally, the modified substrates were immersed in M9 media containing (1–2) × 10⁷ cells ml⁻¹ *E. coli* K-12 or (5–7) × 10⁷ cells ml⁻¹ *P. aeruginosa* bacterial cells for ~ 30 min at 37 °C, after which the substrate was rinsed with fresh M9 solution and Milli-Q water.

2.6. Imaging

Fabricated microarrays were characterized by optical and atomic force microscopy (AFM). Either a Veeco MultiMode SPM or NanoInk, Inc. Nscriptor™ was employed to acquire topography [14], phase, and frictional force images. A cantilever tip (Model # MSCT-AUHW, purchased from Veeco) with a spring constant of 0.05 N m⁻¹ was used for lateral force microscopy (LFM) images while a beam shaped, silicon tapping mode tip with a spring constant of 40 N m⁻¹, from Pacific Nanotechnology, was used for Tapping Mode AFM (TMAFM) imaging. Optical images were obtained with an Axiovert 100A optical microscope equipped with a Penguin 600CL digital camera and StreamPix software. All AFM images were acquired with resolutions of 512 pixels × 512 pixels.

3. Results and discussion

The addition of motile *E. coli* K12 bacterial cells to DPN fabricated MHA dot arrays at pH 6.8 resulted in weak attachment of *E. coli* K12 cells to MHA–PLL modified 2 μm features (figure 1). Optical monitoring of *E. coli* K12 bacterial cell attachment indicates that binding occurred at ~ 30% of the DPN generated MHA–PLL features

under the experimental conditions used and not to the ODT passivated Au surfaces. To further characterize bacterial cell binding to DPN generated MHA–PLL surface arrays, samples containing *E. coli* K12 cells were dried in air, and AFM/LFM studies were conducted. Based on AFM/LFM images, it was confirmed that *E. coli* K12 cells only adhere to the patterned areas but not to passivated portions of the substrate (figure 1). Therefore, DPN generated MHA–PLL modified surfaces, as prepared herein, appear to bind motile *E. coli* K12 bacterial cells.

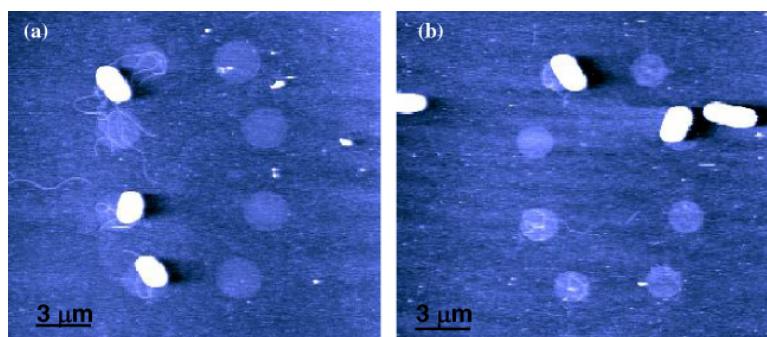


Figure 1. LFM images of two separate ((a) and (b)) DPN generated MHA–PLL dot patterns after the addition of *E. coli* K12 bacteria.

Since it has been proposed that bacterial attachment to MHA–PLL surfaces involves the electrostatic interactions between the negatively charged lipopolysaccharide groups on the surface of bacterial cells and the positively charged amine groups of PLL [19], we hypothesized that the low attachment efficiencies were due to the dense, DPN generated MHA monolayer [7]. It was hypothesized that this dense monolayer results in a decrease in the degree of deprotonation of MHA due to strong hydrogen bonding interactions between surface-bound MHA carboxylate head groups, resulting in weaker electrostatic interactions between MHA and PLL molecules. One way to test this hypothesis is to increase the pH to 9.0 which will increase the degree of MHA deprotonation which, in turn, should increase the electrostatic interaction between MHA and PLL, thereby improving the cellular binding efficiencies. However, at pH 9.0, *E. coli* K12 binding efficiencies increased only moderately to ~ 40%. Therefore, submicron DPN generated MHA dot and line patterns were prepared in order to increase the surface area available for the electrostatic interaction with PLL. An approximately $2\ \mu\text{m} \times 4\ \mu\text{m}$ feature was prepared which was made up of multiple closely spaced dots or lines, allowing PLL to span these surface features.

Initially, various closely spaced MHA dot formations were generated via DPN and tested for motile bacterial attachment (figure 2(a)). These dot formations ranged in total size from 1.5 to $3\ \mu\text{m}$ and were made up of four or seven individual $500\ \text{nm}$ dots of MHA. Figure 3 shows the tapping mode AFM (TMAFM) topographic images of typical DPN patterns composed of MHA. The height of the MHA self-assembled monolayers (SAMs) was found to be $1.61 \pm 0.02\ \text{nm}$ from randomly chosen 20 line profiles. Figure 3(a) shows a height profile drawn across DPN generated MHA patterns on an Au surface. It is clear from the height measurements that DPN generated MHA–SAMs form a close-packed monolayer, in agreement with previous results [12, 20]. These substrates were immersed in a $10\ \text{mM}$ solution of ODT for ~ 30 min, rinsed with ethanol and deionized (DI) water and dried under a stream of nitrogen. A TMAFM topography image of the same features after passivation with ODT and a corresponding height profile are shown in figure 3(b). The apparent thickness of the MHA–SAM decreased to $(0.87 \pm 0.02)\ \text{nm}$. The observed topography signal is likely caused by an imperfection in the SAM of ODT, which is not unexpected since it is well known that ODT requires up to 24 h to achieve a well packed SAM. A layer of PLL was then built on top of the patterned MHA–SAM via a layer-by-layer (LbL) process by exposing MHA substrates to a 0.01% solution of PLL [14]. The selective deposition of a partial PLL layer was confirmed by a change in the height of the DPN features relative to the surrounding area of $0.42\ \text{nm}$ (figure 3(c)).

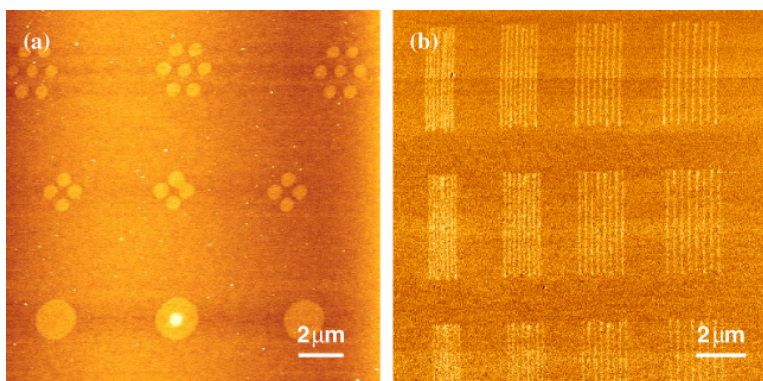


Figure 2. TMAFM topographic images of (a) DPN generated MHA dot patterns and (b) DPN generated MHA/PLL 'block' structures used for bacterial attachment experiments. Scan sizes and scales are $15 \times 15 \mu\text{m}^2$ and 6 nm, respectively. The images were acquired with a frequency of 1 Hz.

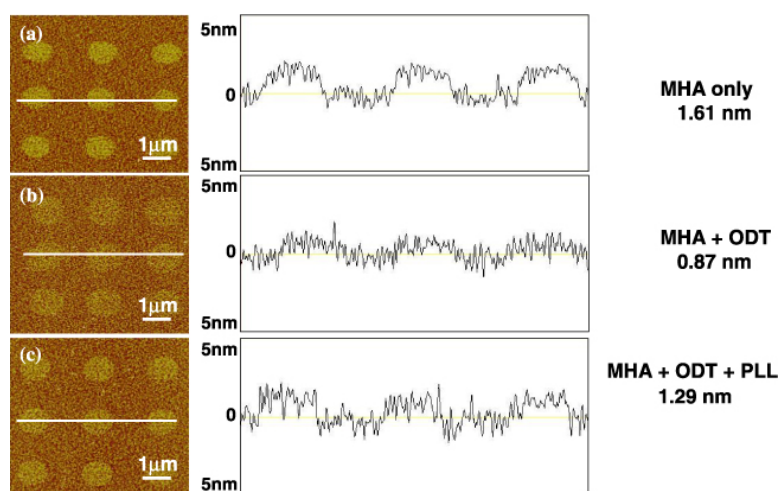


Figure 3. (a) TMAFM topographic image of MHA dot patterns on Au surface and its height profile. The height of the MHA–SAM was determined to be (1.61 ± 0.02) nm. (b) Topographic image of the patterns and corresponding height profile across the DPN features after the remaining Au surface was passivated with ODT molecules. The apparent thickness of the DPN patterns decreased to (0.87 ± 0.02) nm. (c) TMAFM image of the templates and its height profile after the substrates were exposed to a PLL solution. The PLL molecules were selectively built on top of the MHA–SAM only. Scan size and the scale for all the images are $6 \times 6 \mu\text{m}^2$ and 10 nm, respectively.

DPN generated MHA–PLL microarrays were immersed in an aqueous solution of *P. aeruginosa* bacterial cells for ~ 30 min and after extensive rinsing with DI water, characterized optically and via AFM. Typical TMAFM phase images showing attached *P. aeruginosa* bacterial cells are presented in figures 4(a) and (b). It should be noted that the attached *P. aeruginosa* cells survived for over 6 h in an aqueous environment based on direct optical monitoring. *P. aeruginosa* cells were observed bound to individual dots but not to formations consisting of several smaller dots in spite of the similar overall size of the features. The attachment yield remained at $\sim 30\%$, well below the $> 70\%$ level previously observed for PDMS MHA/PLL features [14]. These data, in combination with the change in height of the MHA feature after the addition of PLL, are consistent with the hypothesis that the packing density of the DPN generated MHA–SAMs inhibits the binding of PLL. The distance between the DPN generated MHA dot features was hypothesized to be too large to facilitate PLL to bridge these surface features, which would also make the hydrophobic nature of the passivating agent, ODT, not negligible. This hypothesis is consistent with a change in height of only 0.42 nm after the addition of PLL [14, 19].

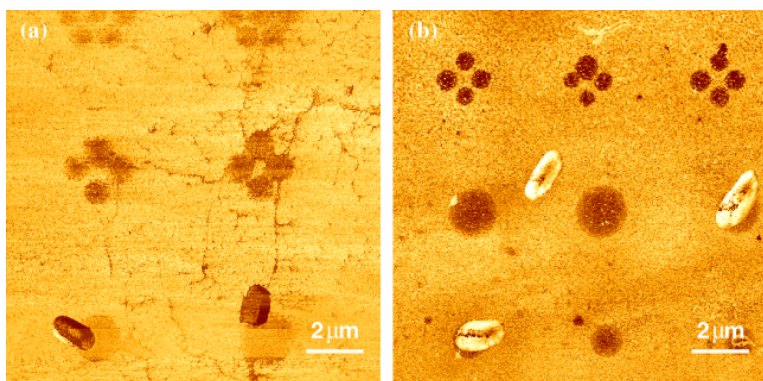


Figure 4. TMAFM phase images of the *P. aeruginosa* bacterial cells attached to the DPN generated templates. The images were collected with scan sizes of $13 \times 13 \mu\text{m}^2$. The cells are attached individually to the MHA/PLL patterns without clustering.

In order to determine if DPN generated MHA microarrays can be generated that will bind PLL and subsequently bacterial cells, 100 nm MHA line pattern 'blocks' were prepared in which the distances between eight lines were systematically changed from 50 to 200 nm (figure 2(b)). The distance between 'blocks' was 3 and 4 μm . TMAFM images of typical DPN generated MHA blocks are shown in figure 5. The height of the MHA-SAM was found to be $1.65 \pm 0.03 \text{ nm}$ averaged from 20 randomly chosen line profiles. After passivation with ODT, the height of the MHA-SAM decreased to $0.92 \pm 0.02 \text{ nm}$, essentially emulating a phase separation process [21]. The height differences between MHA and ODT SAMs for differently spaced lines were found to be identical within error. Next, a layer of PLL was deposited on top of the MHA-SAM by exposing the passivated substrates to a 0.01% solution of PLL. The deposition of PLL to the MHA-SAM was confirmed by a change in the height of the DPN features relative to the surrounding area of 2.31 nm (figures 5(e) and (f)). These data indicate that closely spaced MHA lines offer sufficient electrostatic interaction for PLL molecules to bind to MHA-SAMs and potentially bridge between MHA lines.

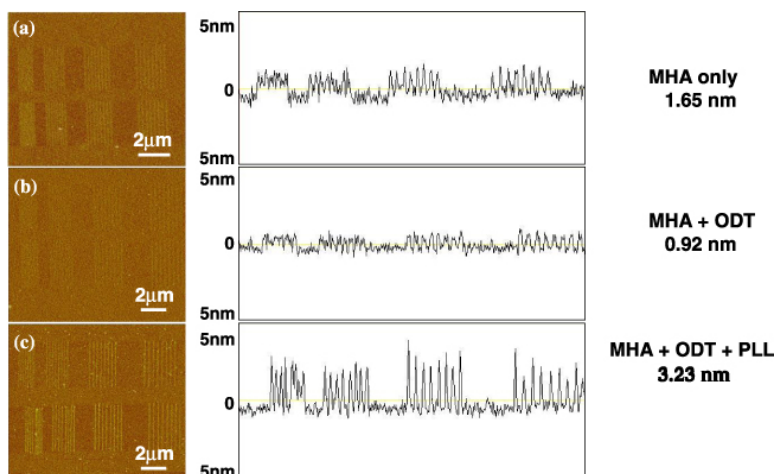


Figure 5. Topographic images of (a) MHA line patterns on the Au surface and its height profile, (b) after backfilling with ODT and its height profile, and (c) after LbL assembly of PLL on MHA features and its height profile. Scan sizes and the scales are $14 \times 14 \mu\text{m}^2$ and 10 nm, respectively. Changes in the apparent thickness of the DPN patterns indicate a successful deposition of each layer.

'Blocks' with 100 nm spacings between lines were used for the attachment of motile *P. aeruginosa* bacterial cells. The MHA/PLL modified templates backfilled with ODT were incubated in an aqueous *P. aeruginosa* bacterial solution for $\sim 30 \text{ min}$ and after extensive rinsing with DI water, were characterized both optically and via AFM. Typical TMAFM phase images showing attached *P. aeruginosa* bacterial cells are presented in

figures 6(a) and (b). It should be noted that the attached *P. aeruginosa* cells survived for > 6 h in an aqueous environment based on direct optical monitoring. *P. aeruginosa* cells were observed bound to individual 'blocks' with an attachment yield of > 70%. Motile *P. aeruginosa* cells mostly attached through their body rather than their flagellum, suggesting an electrostatic interaction between the cell body and the MHA/PLL microarray is the predominant immobilization process.

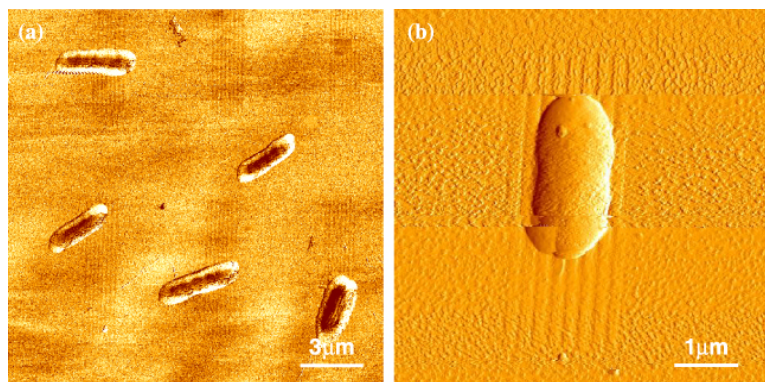


Figure 6. TMAFM phase images of the *P. aeruginosa* bacterial cells attached to the DPN generated templates. Scan sizes are (a) $18 \times 18 \mu\text{m}^2$ and (b) $6 \times 6 \mu\text{m}^2$. The attachment of the bacterial cells is directed by the pre-programmed templates.

In conclusion, motile *P. aeruginosa* bacterial cells can be attached to DPN generated MHA/PLL 'block' surface structures via an electrostatic interaction between negatively charged groups of the bacterial cell surface with positively charged PLL assemblies. Cellular attachment to pre-designed DPN generated microarrays was found to be dependent on the shape and size of the surface feature. While this observation is likely due in part to dense, well formed MHA monolayers generated via DPN, it may also simply be due to the physical shape of the surface structure. These data indicate that 'block' surface structures provide a promising footprint for the attachment of motile bacterial cells that may find utility in cell based biosensors or single cell studies.

Acknowledgments

This work was supported by the National Science Foundation (CHE-0652981, RCH) and the Air Force Office of Scientific Research (F49620-03-1-0382, RCH).

References

- [1] Rosi N L and Mirkin C A 2005 *Chem. Rev.* **105** 1547
- [2] Sarikaya M, Tamerler C, Schwartz D T and Baneyx F 2004 *Ann. Rev. Mater. Res.* **34** 373
- [3] Medintz I 2006 *Nat. Mater.* **5** 842
- [4] Mershin A, Cook B, Kaiser L and Zhang S 2005 *Nat. Biotechnol.* **23** 1379
- [5] Houseman B T and Mrksich M 2002 *Chem. Biol.* **9** 443
- [6] Wilson D L, Martin R, Hong S, Cronin-Golomb M, Mirkin C A and Kaplan D L 2001 *Proc. Natl Acad. Sci.* **98** 13660
- [7] Ginger D S, Zhang H and Mirkin C A 2004 *Angew. Chem. Int. Edn* **43** 30
- [8] Chovan T G A 2002 *Trends Biotechnol.* **20** 116
- [9] Mrksich M 2002 *Curr. Opin. Chem. Biol.* **6** 794
- [10] Bucci C, Lavitola A, Salvatore P, Del Giudice L, Massardo D R, Bruni C B and Alifano P 1999 *Mol. Cell* **3** 435
- [11] Ostuni E, Yan L and Whitesides G M 1999 *Colloids Surf. B* **15** 3
- [12] Piner R D, Zhu J, Xu F, Hong S and Mirkin C A 1999 *Science* **283** 661
- [13] Salaita K, Wang Y H, Fragala J, Vega R A, Liu C and Mirkin C A 2006 *Angew. Chem. Int. Edn* **45** 7220
- [14] Rozhok S, Clifton K F, Shen F, Littler P H, Fan Z, Liu C, Mirkin C A and Holz R C 2005 *Sma II* **1** 445

- [15] Fine M J, Smith M A, Carson C A, Mutha S S, Sankey S S, Weissfeld L A and Kapoor W N 1996 *J. Am. Med. Assoc.* **275** 134
- [16] Diekema D J, Pfaller M A, Jones R N, Doern G V, Winokur P L, Gales A C, Sader H S, Kugler K and Beach M 1999 *Clin. Infect. Dis.* **29** 595
- [17] Ferrández A, Hawkins A C, Summerfield D T and Harwood C S 2002 *J. Bacteriol.* **184** 4374
- [18] Jang J, Hong S, Schatz G C and Ratner M A 2001 *J. Chem. Phys.* **115** 2721
- [19] Rozhok S, Fan Z, Nyamjav D, Liu C, Mirkin C A and Holz R C 2006 *Langmuir* **22** 11251
- [20] Rozhok S, Piner R D and Mirkin C A 2003 *J. Phys. Chem.* **107** 751
- [21] Salaita K, Amarnath A, Maspoch D, Higgins T B and Mirkin C A 2005 *J. Am. Chem. Soc.* **127** 11283